Earth and Planetary Science Letters 601 (2023) 117904

Contents lists available at ScienceDirect

Earth and Planetary Science Letters

journal homepage: www.elsevier.com/locate/epsl

Ancient alluvial plains at Oxia Planum, Mars

Joel M. Davis [a,*], Matthew R. Balme [b], Peter Fawdon [b], Peter M. Grindrod [c], Elena A. Favaro [b], Steven G. Banham [d], Nicolas Thomas [e]

[a] Department of Earth and Planetary Sciences, Birkbeck, University of London, London, WC1E 7HX, UK
[b] School of Physical Sciences, The Open University, Milton Keynes, Buckinghamshire, MK7 7EA, UK
[c] Department of Earth Sciences, Natural History Museum, London, SW7 5BD, UK
[d] Department of Earth Sciences and Engineering, Imperial College London, London, SW7 2AZ, UK
[e] Physikalisches Institut, University of Bern, Sidlerstrasse 5, 3012 Bern, Switzerland

ARTICLE INFO

Article history:
Received 1 August 2022
Received in revised form 27 October 2022
Accepted 1 November 2022
Available online 21 November 2022
Editor: J.-P. Avouac

Keywords:
Mars
remote sensing
geomorphology
surface processes
landing sites
planetary science

ABSTRACT

The geologic origin of the ancient, phyllosilicate-bearing bedrock at Oxia Planum, Mars, the ExoMars rover landing site, is unknown. The phyllosilicates record ancient aqueous processes, but the processes that formed the host bedrock remain elusive. Here, we use high-resolution orbital and topographic datasets from the HiRISE, CaSSIS and CTX instruments to investigate and characterize fluvial sinuous ridges (FSRs), found across the Oxia Planum region. The FSRs form segments up to 70 km long, are 20-600 m wide, and up to 9 m in height, with sub-horizontal layering common in ridge margins. Some FSRs comprise multi-story ridge systems; many are embedded within the phyllosilicate-bearing bedrock. We interpret the FSRs at Oxia Planum as deposits of ancient, episodically active, alluvial river systems (channel-belt and overbank deposits). Thus, at least some of the phyllosilicate-bearing bedrock was formed by ancient alluvial rivers, active across the wider region, though we do not exclude other processes from contributing to its formation as well. The presence of alluvial floodplains at Oxia Planum increases the chances of the ExoMars rover detecting signs of ancient life. Future exploration by the ExoMars rover can verify the alluvial interpretation and provides an opportunity to investigate some of the oldest river deposits in the Solar System.

1. Introduction and the geology of Oxia Planum

The main objective of the European Space Agency (ESA) ExoMars "Rosalind Franklin" rover mission is to search for evidence of past life on Mars (Vago et al., 2017). Noachian-aged, phyllosilicate-bearing bedrock exposures at Oxia Planum, the landing site for the mission (Quantin et al., 2021), forms the main sampling target as it provides strong evidence for ancient aqueous processes and could potentially preserve organic material (Westall et al., 2015). Although the phyllosilicates are widespread across the landing site, it is unclear whether they are authigenic and/or detrital, or what processes formed the host bedrock (Quantin et al., 2021; Mandon et al., 2021). Understanding the depositional process that formed these rocks and the paleo-environmental conditions under which they were laid down, is critical for mission success. Although landing sites for previous missions have been proposed at the nearby and similarly ancient Mawrth Vallis (Grant et al., 2011, 2018), no rover mission has ever visited a region on Mars as old as Oxia Planum.

Oxia Planum itself comprises a shallow topographic basin, situated on the margin of hemispheric dichotomy of Mars, which divides the highlands of Arabia Terra to the southeast from the Chryse Planitia lowlands to the northwest (Fig. 1). The boundaries of the Oxia basin may demarcate an ancient, highly degraded impact structure (Fawdon et al., 2021). The depth of the phyllosilicate-bearing bedrock basin fill is unknown, but is at least 100 m in some areas (Quantin et al., 2021). The Oxia Planum Fe/Mg phyllosilicates are part of the regionally extensive circum-Chryse phyllosilicates, which are best exposed at Mawrth Vallis (e.g., Noe Dobrea et al., 2010; Loizeau et al., 2007). Sub-horizontal, meter-scale layering, exposed in the phyllosilicate-bearing bedrock at Oxia Planum generally points to a sedimentary origin, although multiple formation hypotheses for the bedrock are also possible, including: large scale lava flows, volcaniclastic deposits, impactogenic materials, aeolian deposits, or fluvio-lacustrine deposits (Quantin et al., 2021; Mandon et al., 2021). Combined observations from the High Resolution Imaging Science Experiment (HiRISE; McEwen et al., 2007), Colour and Stereo Science Imaging System

* Corresponding author.
E-mail address: joel.davis@bbk.ac.uk (J.M. Davis).

https://doi.org/10.1016/j.epsl.2022.117904

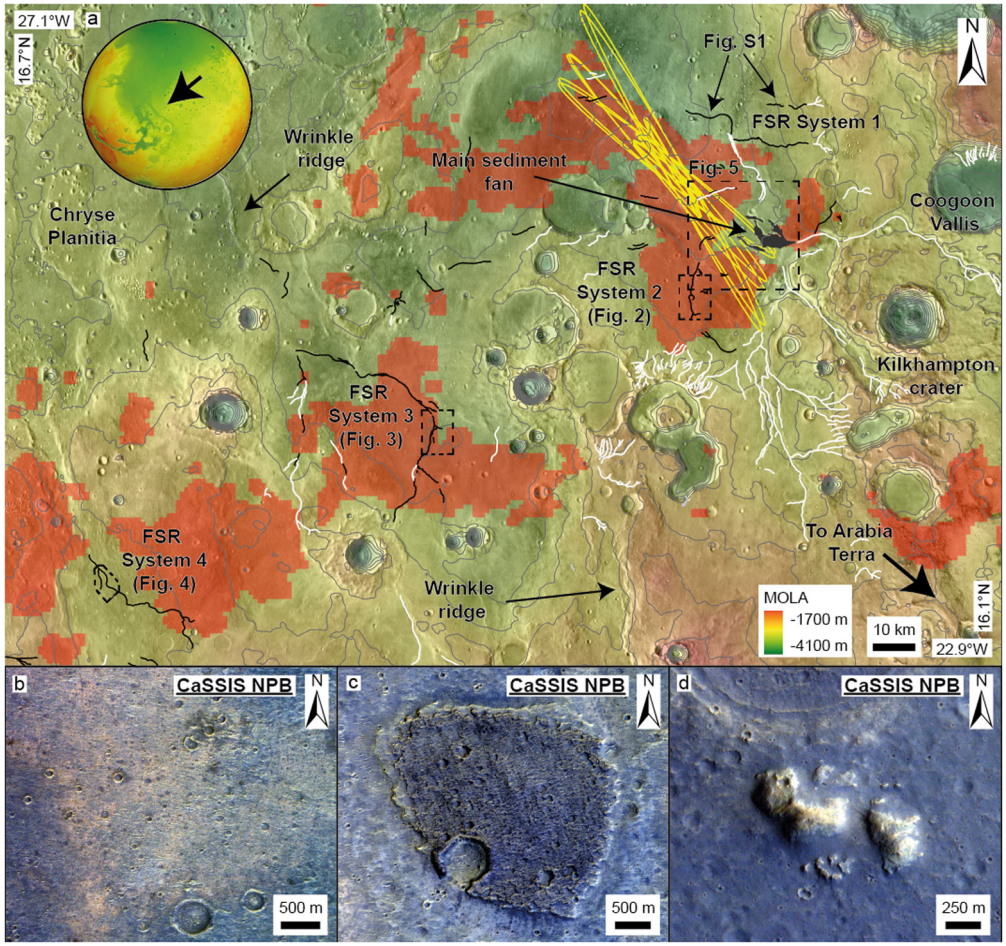

Fig. 1. (a) MOLA topographic map showing the distribution of fluvial sinuous ridges (FSRs; black solid lines) and fluvial valleys (white lines) in the Oxia Planum region. Detections of phyllosilicate minerals are shown in red (modified from Quantin et al., 2021). The ExoMars 2022 landing ellipses are shown in yellow. Contours shown at 100 m intervals as fine grey lines. (b) CaSSIS image showing the phyllosilicate-bearing bedrock at Oxia Planum. (b) CaSSIS image of dark, crater-retaining unit. (c) CaSSIS image of light-toned mounds. Both the dark, crater-retaining unit and the light-toned mounds overlie the phyllosilicate-bearing bedrock. All image IDs for figures are provided in Table S2. (For interpretation of the colors in the figure(s), the reader is referred to the web version of this article.)

(CaSSIS; Thomas et al., 2017) and the Compact Reconnaissance Imaging Spectrometer for Mars (CRISM; Murchie et al., 2007) divide the phyllosilicate-bearing bedrock at Oxia Planum into at least two distinct sub-units, which may reflect compositional variations: an underlying, orange-toned unit and an overlying, more olivine-rich, blue-toned unit (Mandon et al., 2021; Parkes Bowen et al., 2022).

At the eastern margins of the Oxia Planum landing ellipse is a 10 km long sediment fan (Fig. 1), previously interpreted as a delta, which likely formed in multiple stages (Quantin et al., 2021; Molina et al., 2017). The fan is sourced from a regional highland catchment to the southeast, including the extensive and long-lived Coogoon Vallis system (Fawdon et al., 2022; Molina et al., 2017). The fan illustrates how fluvial processes might have transported detrital phyllosilicates from the highland catchment into Oxia Planum, but is interpreted to postdate the formation of the phyllosilicate-bearing bedrock (Quantin et al., 2021; Mandon et al., 2021). Two additional, geologically younger materials are found at Oxia: a dark-toned, crater-retaining unit and a series of light-toned mounds. Both were probably once more extensive, suggesting that the entire region has been subject to widespread and severe erosion (Quantin et al., 2021; McNeil et al., 2021). The dark crater-retaining unit has previously been interpreted as an early Amazonian-age volcanic unit (Quantin et al., 2021). The paleosurface now represented by the mounds is constrained by regional stratigraphic relationships to have formed in the early to middle Noachian (McNeil et al., 2021).

Fawdon et al. (2022) identified several fluvial sinuous ridges (FSRs) in the Oxia basin, providing further evidence for fluvial activity near the landing site. FSRs, or "inverted channels", are ridges of indurated, fluvially deposited sediment exhumed by differential erosion (e.g., Burr et al., 2010; Williams et al., 2009; Davis et al., 2016). Examples on both Earth and Mars demonstrate that FSRs may comprise either a single system channel-fill or deposits of migrating and aggrading river channel-belts (e.g., Hayden et al., 2019; Davis et al., 2019; Balme et al., 2020; Zaki et al., 2021). The latter are particularly relevant for understanding paleo-environmental conditions as they may record multiphase depositional events over geologic timescales. Having testable hypotheses ahead of the ExoMars rover landing is critical for any time-limited investigations of the fluvial sinuous ridges performed on the surface. Here, we explore the processes that the FSRs may record, their relationship to the phyllosilicate-bearing bedrock, and the implications of their existence for its origin.

2. Data and methods

We investigated FSRs in Oxia Planum using orbital datasets including HiRISE (McEwen et al., 2007), CaSSIS (Thomas et al., 2017), and Context Camera (CTX; Malin et al., 2007) image and topographic datasets. We mapped the distribution of potential FSRs

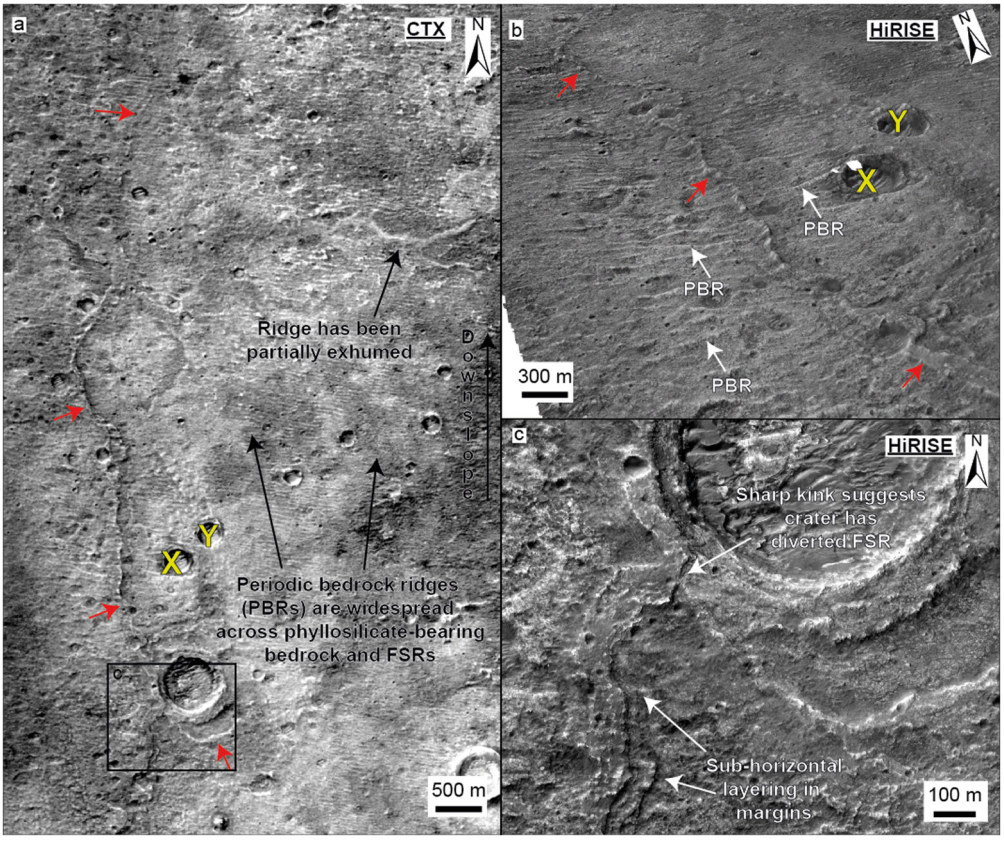

Fig. 2. CTX and HiRISE images of FSR 2, south of the Oxia Planum landing ellipse. (a) CTX image showing ~10 km section of FSR (highlighted by red arrows). There are several examples of smaller ridges partially exhumed from the phyllosilicate-bearing bedrock. (b) Oblique, 3D HiRISE view of FSR (highlighted by red arrows) facing northeast (note X and Y are the same as in (a)). PBRs have eroded into both the phyllosilicate-bearing bedrock and the FSR. DEM constructed from ESP_069815_1975 and ESP_072017_1975. (c) HiRISE image showing section of FSR with a sharp kink around the impact crater, suggesting paleo-flow conformed to topography.

in the vicinity of Oxia Planum onto a CTX mosaic basemap (6 m/pix) and accompanying digital elevation model (DEM; 20 m/pix; Fawdon et al., 2021). Our mapping was supplemented by georeferenced HiRISE and CaSSIS images where available and we built on the earlier map of Fawdon et al. (2022). We investigated the morphology of the FSRs using a combination of panchromatic CTX images, infrared-red-blue (IRB) and red only HiRISE images (0.25 m/pix), and near infrared-panchromatic-blue (NPB) false color CaSSIS images (4.5 m/pix). Where possible, we generated additional HiRISE and CTX DEMs using the USGS Integrated Software for Imagers and Spectrometers (ISIS) software and the BAE photogrammetric package SOCET SET (Kirk et al., 2008). In cases where SOCET SET failed to produce the DEM, we used the NASA Ames Stereo Pipeline (Beyer et al., 2018). DEMs were tied to Mars Orbital Laser Altimeter (Zuber et al., 1992) topography and exported with a post spacing of 20 m/pixel and 1 m/pixel for CTX and HiRISE, respectively. These DEMs were supplemented with MOLA topography (463 m/pix).

3. Observations

3.1. Catchment and morphology of FSR systems

We define four FSR systems (from northeast to southwest, 1-4; Fig. 1). They each drain a region separate to the larger Coogoon Vallis catchment, which connects to the eastern sediment fan (Fawdon et al., 2022). FSR system 1 is found within the eastern part of the landing ellipse; all other systems occur south or southwest of the landing site, but in the same assemblage of geologic materials. All four FSR systems also share the same morphologic characteristics: they are straight to sinuous (sinuosity 1-1.4), tens to hundreds of meters wide (range is 20-600 m), and morphologically highly degraded (Figs. 2, 3). Where suitable CTX or HiRISE topography was available, the FSRs were measured to be 1-9 m above the adjacent bedrock. The FSRs are mostly found in contiguous to semi-contiguous segments; the longest individual segment is ~70 km. The FSRs are usually set within low relief plains or in subtle (meters deep), approximately kilometer-wide valleys, and are often found downslope of more well-defined erosional valleys (Figs. 2, 3, 4, S1). The ridge trends are perpendicular to contour lines, with their upslope ends being 100-200 m higher in elevation than the downslope ends (Fig. 1). The inferred paleoflow directions are broadly to the north or northwest, towards Chryse Planitia, where the FSRs eventually become unrecognizable. Sub-horizontal, meter-scale layering is clearly present in the margins of the FSRs, and grades into the adjacent and underlying terrain (i.e., the phyllosilicate-bearing bedrock; Figs. 2, 3). Beyond this, there is no discernable sedimentary architecture recognizable in FSR margins at the scale of the available data.

3.2. Relationship of FSRs to the surrounding terrain

A comparison of the FSR locations and previous detections of phyllosilicates in Oxia Planum (Carter et al., 2015; Quantin et al., 2021) demonstrates significant overlap (Fig. 1). Most of the main and peripheral FSR systems are situated on or near detections of phyllosilicates. However, due to the limits of orbital detections, phyllosilicates are likely to be more abundant across the region than shown in Fig. 1 (Murchie et al., 2007); certainly, the morphological characteristics of the phyllosilicate-bearing bedrock (e.g., light-toned, sub-horizontal layering, fractured) can be seen across areas that extend far beyond those with spectral phyllosilicate sig-

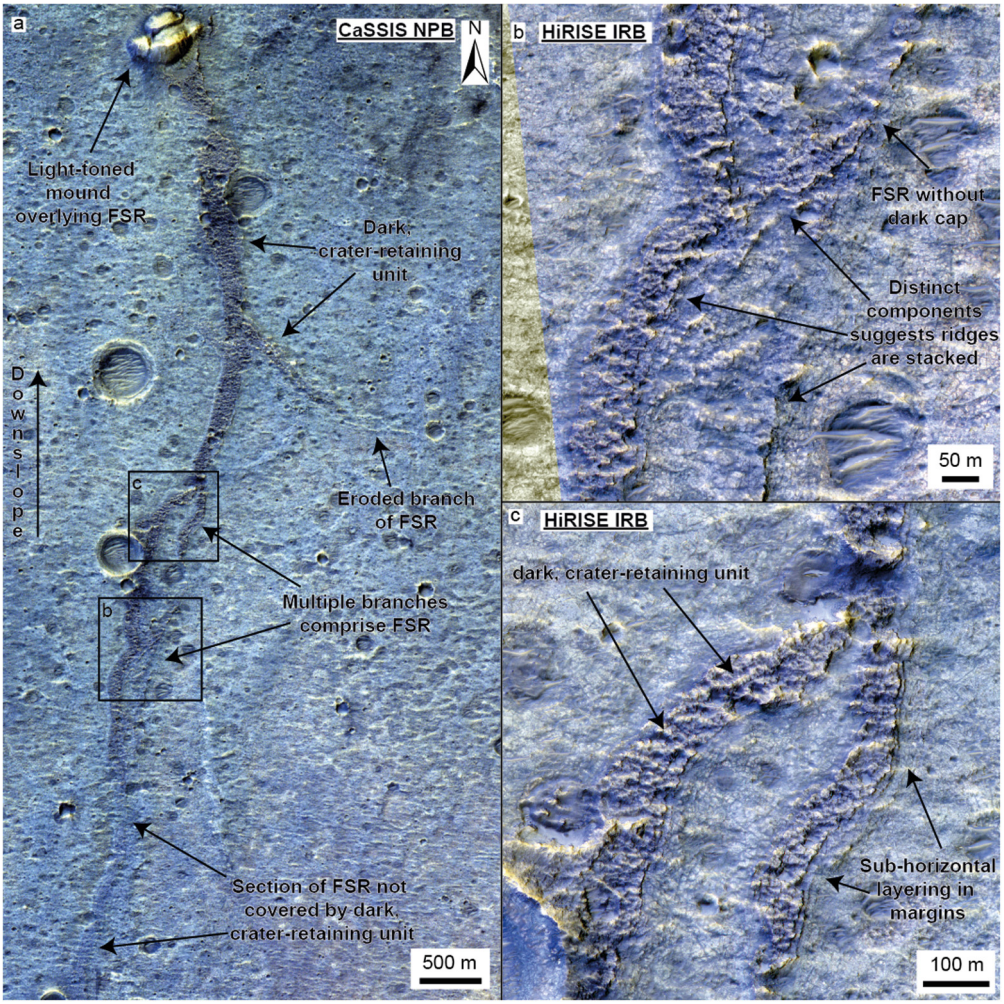

Fig. 3. CaSSIS and HiRISE images of FSR System 3 southwest of Oxia Planum landing ellipse. (a) CaSSIS NPB image showing FSR with multiple branches set within the phyllosilicate-bearing bedrock. (b) HiRISE IRB image showing section of FSR. Here, multiple vertically stacked ridges are present and in places, the FSR is not covered by the dark crater-retaining unit. (c) HiRISE IRB showing section of FSR covered by dark, crater-retaining unit. However, sub-horizontal layering is still visible in the FSR margins.

natures (Quantin et al., 2021; Mandon et al., 2021). CaSSIS NPB and HiRISE IRB images reveal that the FSRs are generally confined to the blue-toned (stratigraphically higher) sub-unit of the phyllosilicate-bearing bedrock (Fig. 3). Many FSR systems appear partially exhumed from within the phyllosilicate-bearing bedrock (Fig. 2, 3). Periodic bedrock ridges (PBRs; Montgomery et al., 2012), parallel sets of aeolian-formed ridges eroded into bedrock, previously identified across large parts of the phyllosilicate-bearing bedrock at Oxia Planum (Silvestro et al., 2021; Favaro et al., 2021), are also superposed on several FSR systems and the adjacent bedrock (e.g., Fig. 2). Recently, bedrock ridges were also observed by the Curiosity rover at Glen Torridon in Gale crater, and similarly interpreted as PBRs (Stack et al., 2022). FSR system 2, south of the landing site is overlain by the eastern sediment fan (Fig. 5).

Generally, FSR pathways conform to the local topography, except where they are deformed by tectonic wrinkle ridges; there are examples of FSRs converging on degraded impact craters, only to be sharply diverted around them on approach (Fig. 2c). Additionally, shallow, degraded, impact craters (typically < 500 m diameter), which have formed into the phyllosilicate-bearing bedrock adjacent to the FSRs, are commonly infilled (Fig. 6). In some cases, the infill comprises light-toned, concentric layered deposits (Figs. 6b, c, e, f); in others, craters have been filled and/or buried almost entirely (Fig. 6d). Similar infill is not present in less degraded, fresher impact craters (i.e., those with preserved ejecta and well-defined rims). Some of the FSR systems appear covered by the regionally recurrent, dark crater-retaining unit (Quantin et al., 2021). However, we note that (1) this coverage is not continuous along the entire length of FSRs and (2) in places, the dark crater-retaining unit has been eroded back, revealing a distinct, underlying ridge structure (Fig. 3). This is particularly apparent in CaSSIS and HiRISE images (Fig. 3). Like other examples, these FSRs also bear similarities in tone, color, and texture, to the phyllosilicate-bearing bedrock, while the dark crater-retaining unit generally appears to be of limited vertical thickness (we estimate $\sim$1 m or less, but this is at the limit of what we can measure vertically using our HiRISE DEMs. We note that this is also the case for other regional examples of FSRs, outside of Oxia Planum. One example, FSR system 3, is superposed by light-toned mounds (McNeil et al., 2021), potentially putting a lower age limit on FSR formation (Fig. 3; i.e., middle Noachian or younger).

4. Discussion

4.1. Interpretation of the fluvial sinuous ridges

We interpret the FSRs as exhumed fluvial deposits. The FSRs are morphologically distinct from large-scale tectonic wrinkle ridges (e.g., Andrews-Hanna, 2020), which have deformed the region and do not generally conform to regional topographic trends. Also, there are no recognizable glacial landforms associated with the FSRs, making an esker interpretation unlikely (Butcher et al., 2021).

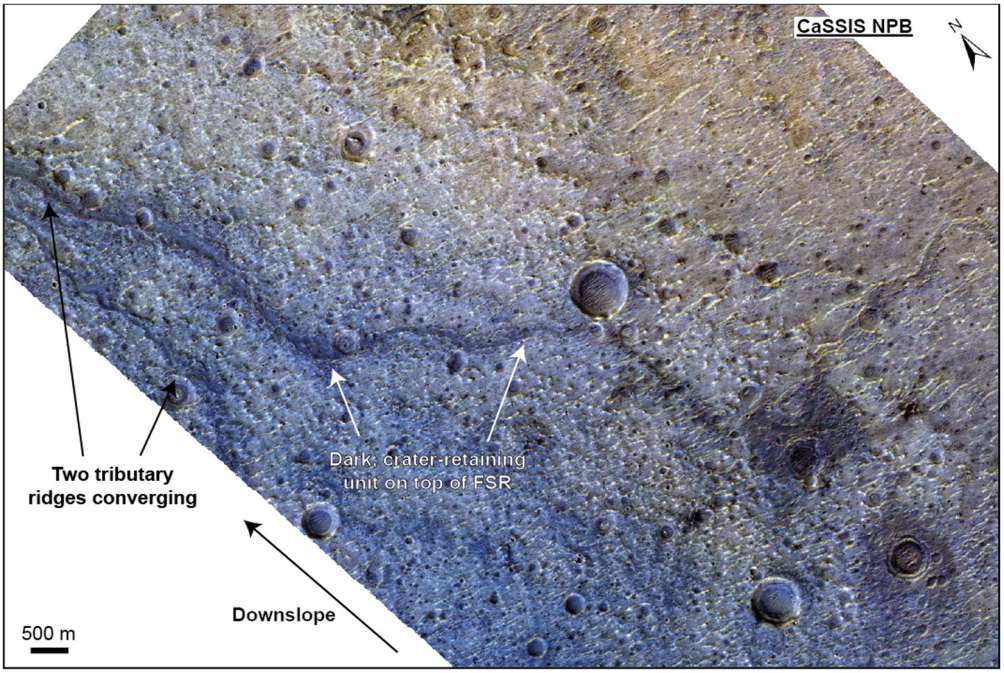

Fig. 4. Planview CaSSIS NPB mosaic showing part of FSR System 4, approximately 160 km southwest of the Oxia Planum landing site. Like FSR System 3, the ridge is covered by the dark, crater-retaining unit.

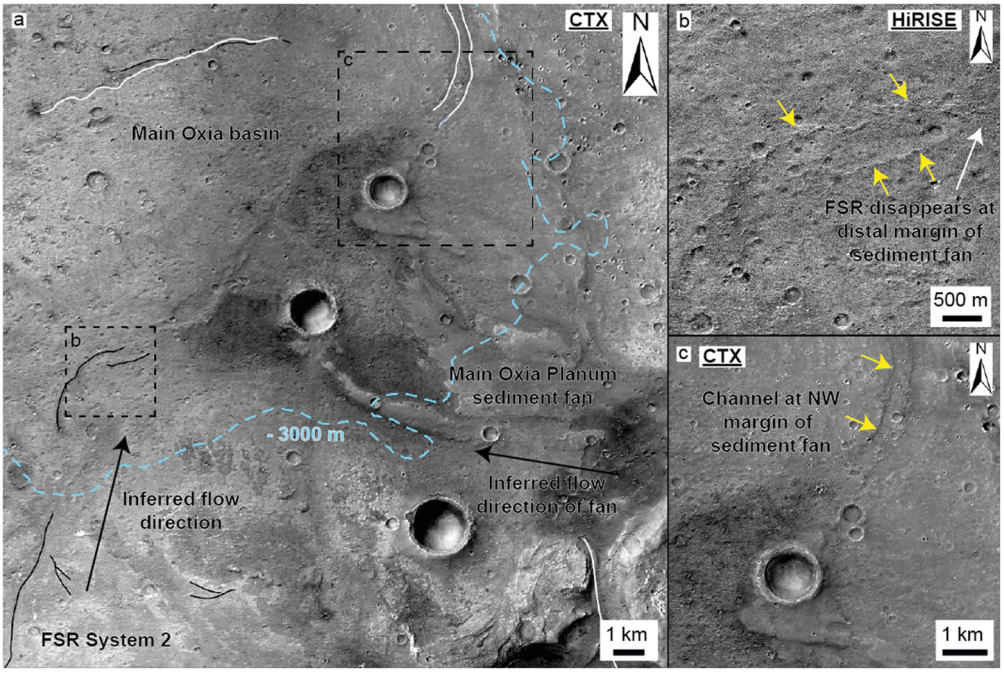

Fig. 5. (a) CTX mosaic showing the delta-like sediment fan at the eastern margin of Oxia Planum. The inferred paleo-flow direction of FSR system 2 contrasts with that of the delta-like sediment fan. Negative relief channels are shown by white lines, FSRs are shown by black lines. (b) HiRISE image showing that FSR system 2 (yellow arrows) disappears as it approaches the distal margin of the sediment fan, suggesting it is buried by the fan. (c) CTX image showing a channel (yellow arrows) emerging at the NW margin of the sediment fan, possible a continuation of FSR system 2.

We note that no FSRs are set within deep, erosional valleys; instead, they are found on low-relief plains (the phyllosilicate-bearing bedrock; Figs. 2, 3, 4, S1a) or set within or downslope of shallow valleys (Figure S1b). The FSRs therefore likely represent the deposits of ancient, alluvial river systems that traversed the plains at and around Oxia Planum (e.g., Hayden et al., 2019; Davis et al., 2019; Balme et al., 2020; Zaki et al., 2021), rather than erosive rivers incised into bedrock. Secondary ridges associated with and converging on the main systems could be either tributaries or earlier generations of rivers which are in different states of exhumation, or both.

The sub-horizontal layering in the FSRs (Figs. 2, 3) and examples of both partially exhumed and superposing ridge systems (i.e., ridge stacking; Fig. 3b) argues against simple channel-fill, deposited in a single event, composing the ridges. These characteristics instead support an interpretation of the FSRs as the remains

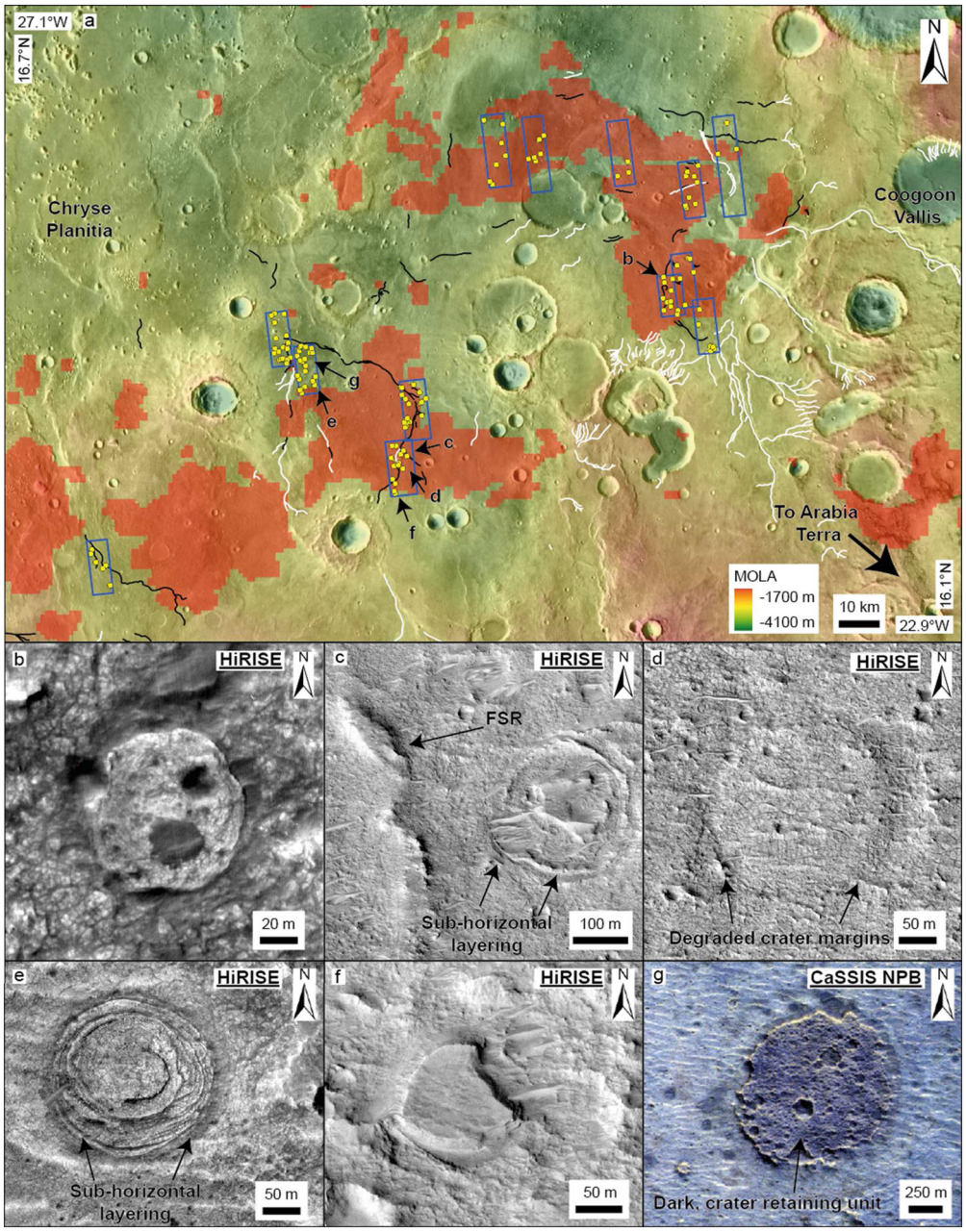

Fig. 6. (a) MOLA topographic map showing distribution of degraded craters within the phyllosilicate-rich bedrock that have been infilled with light-toned layered deposit, and in some cases, buried almost entirely (yellow circles). We mapped the distribution of these features across 13 select HiRISE images of the phyllosilicate-rich bedrock. Detections of phyllosilicate minerals are shown in red (modified from Quantin et al., 2021). Higher concentrations of infilled craters generally occur in proximity to the FSRs (black lines). (b - f) HiRISE and CTX images showing light-toned layered material in degraded impact craters, which may represent sediment deposits formed in an alluvial or shallow lacustrine setting. (g) CaSSIS NPB image showing inverted crater composed of the dark, crater-retaining unit. Note we did not include these features in (a) as the formation of the dark, crater-retaining unit postdates the formation of the phyllosilicate-rich bedrock.

of channel-belt and floodplain deposits. The concentric layered deposits in impact craters adjacent to the FSRs may record overbank deposition and/or ponding in local accommodation (Fig. 6). Some of the FSRs have previously been interpreted as erosional channels that were later and exclusively filled by the dark crater-retaining unit (i.e., non-fluvially deposited material; Quantin et al., 2021). However, the observations that this material is generally thin (~1 m or less) and, in places, has been eroded back to reveal a distinct, underlying, layered ridge structure, invalidates this interpretation in at least these examples (Fig. 3). Instead, most of the ridge structure of the FSRs appears to be embedded within and exhumed from the phyllosilicate-bearing bedrock itself (Figs. 2, 3).

4.2. Constraints on phyllosilicate-bearing bedrock formation

We note that most of the FSRs are found outside the landing ellipse (Fig. 1). However, due to the inherent nature of migratory river systems and the erosional processes that expose them in the rock record, it is unlikely that the FSRs as they are currently exposed represent the full extent of alluvial river systems at Oxia Planum, both spatially and vertically within the stratigraphy. Furthermore, the similar morphological characteristics on the phyllosilicate-bearing bedrock throughout the region points to common formational processes. Thus, we suggest that at least some of the phyllosilicate-bearing bedrock comprises alluvial (both channel-belt and floodplain) deposits, which developed as self-

formed alluvial plains; this may be the case throughout the landing ellipse and the wider region. The low relief (<10 m) and poor exposure of the FSRs across the Oxia Planum landscape may be due to a high mudstone fraction in the bedrock, which led to moderate differential erosion producing more subdued topography than is typical of other landscapes containing FSRs (e.g., Davis et al., 2019; Zaki et al., 2021). The FSR height (1-9 m) reveals the minimum vertical thickness of alluvial deposits at Oxia Planum; the true thickness of alluvial deposits is likely be greater. These ancient rivers provide one mechanism for the erosion, transport, and deposition of sediment in Oxia Planum. The upland catchment from which these rivers seem to originate (Fawdon et al., 2022), and the presence of impact craters which have altered their pathways within Oxia Planum, suggest that sediment was sourced both regionally in the highlands and locally from the phyllosilicate-bearing bedrock itself, before being deposited elsewhere.

The presence of embedded and partially filled impact craters in the phyllosilicate-bearing bedrock (Fig. 6) points to substantive hiatuses in bedrock deposition and the formation of paleo-surfaces (e.g., Kite et al., 2017), followed by a later resumption in depositional processes. Thus, if alluvial river systems were responsible for the deposition of sedimentary bedrock here, they were probably episodically active, although the presence of stacked channel deposits (e.g., Fig. 3) suggests these episodes consisted of sustained aggradation (Colombera et al., 2015). The association of the FSRs with the blue-toned sub-unit of the phyllosilicate-bearing bedrock, is consistent with episodic activity, where the presence of olivine points to limited aqueous alteration (Mandon et al., 2021). Furthermore, Fawdon et al. (2022) identified two major phases of fluvial activity separated by a substantial hiatus in the regional Coogoon Vallis system. Our interpretation does not constrain the origin of the phyllosilicates themselves as detrital or authigenic. If phyllosilicate-bearing sediments were present when these ancient river systems were active, the phyllosilicate minerals might have contributed to the stability of their banks (e.g., Lapôtre et al., 2019). Our alluvial hypothesis does not exclude other sources of sediment playing a role in building the terrain as well (e.g., volcaniclastic, aeolian, impactogenic; Quantin et al., 2021; Mandon et al., 2021). If this is the case, the phyllosilicate-bearing bedrock may comprise alluvial deposits interbedded with other facies. It is possible that the wider, regional phyllosilicate-bearing bedrock across Chryse Planitia and Mawrth Vallis (e.g., Noe Dobrea et al., 2010; Loizeau et al., 2007) may also have had an alluvial origin; the presence of FSRs in these regions would help constrain this hypothesis.

4.3. Testing the alluvial hypothesis with the ExoMars rover

Our interpretation of an ancient alluvial environment can be reconciled with the former presence of a standing body of water at Oxia Planum, previously interpreted from the presence of a delta-like sediment fan at the end of Coogoon Vallis (Quantin et al., 2021; Molina et al., 2017). It is likely that these different paleo-environments existed at separate times; indeed, Quantin et al. (2021) suggest the delta-like sediment fan formed after the phyllosilicate-bearing bedrock (which contains the FSRs). Furthermore, investigations of terrestrial FSRs have shown that they can record multiple paleo-environments not apparent in planimetric pattern. For example, in the Californian Mojave Desert, Miller et al. (2018) document multiple examples of lake-rise pulses contained within inverted paleochannels (i.e., FSRs) associated with the southern Lake Coyote in the late Quaternary. The lake-rise pulses cover a period of ~10 ka and were identified from radiocarbon dating of lacustrine fossils, but importantly were not recognizable in the ridge structure from orbital data (Miller et al., 2018). A similar scenario at Oxia Planum is possible and evidence for lacustrine episodes recorded within the FSRs might only be revealed by in situ investigations.

Our predictions of an ancient alluvial landscape in Oxia Planum can be readily tested by the ExoMars rover. If widespread alluvial plains are present at Oxia Planum, diagnostic outcrops and lithologies such as conglomerates may be present. This is the case in the plains surrounding Mount Sharp in Gale crater, as imaged by the Curiosity rover (Williams et al., 2013; Grotzinger et al., 2014), despite there being little evidence of an ancient alluvial environment from orbital data. If, for example, similar fine-pebble conglomerates (2-40 mm coarse grain size range) occur at the Oxia Planum landing site, they would be identifiable at working distances of up to 50 m by ExoMars' Panoramic Camera instrument, using its High Resolution Camera (Coates et al., 2017). Grain sizes measured from such outcrops could be used for paleo-hydrologic reconstructions (Williams et al., 2013), potentially revealing Noachian surface flow conditions. Additionally, the capability of the ExoMars rover to drill to 2 m depth into bedrock (Vago et al., 2017) would potentially allow the rover to investigate facies variation with depth, testing our alluvial interpretation of the bedrock. Sub-surface investigations could be supported by the rover's ground penetrating radar, the Water Ice Subsurface Deposit Observation on Mars instrument (Ciarletti et al., 2017).

An ancient alluvial environment would provide the opportunity for the ExoMars rover to investigate the development of apparent bank-stable rivers in the absence of vegetation, a major outstanding question in pre-Cambrian geology (e.g., Lapôtre et al., 2019). Due to the rapid burial of sediment, alluvial floodplains and lacustrine environments are considered to have moderate to high preservation potential for organic matter (Summons et al., 2011). Thus, as phyllosilicate-bearing bedrock with morphology identical to the FSR-bearing surface shown here is widespread in the landing ellipse, our interpretation increases the likelihood that the ExoMars rover will encounter habitable paleoenvironments and meet its main mission objective of detecting ancient life. Finally, given the ancient age of the phyllosilicate-bearing bedrock (~4 Ga; Quantin et al., 2021), if the alluvial hypothesis is correct, the ExoMars rover may provide the opportunity to investigate in situ some of the oldest preserved river deposits in the Solar System.

CRediT authorship contribution statement

Joel M. Davis and Matthew R. Balme are responsible for the conceptualization, funding acquisition, formal analysis, investigation, and writing the manuscript. Peter Fawdon is contributed to the formal analysis, supplying data, and editing the manuscript. Peter M. Grindrod, Elena A. Favaro, and Steven G. Banham contributed to the review and editing of the manuscript. Nicolas Thomas contributed resources and to the writing and editing of the manuscript.

Declaration of competing interest

The authors declare that they have no known competing financial interests or personal relationships that could have appeared to influence the work reported in this paper.

Data availability

The standard data products used here are available from the NASA Planetary Data System as follows. (1) HiRISE: https://hirise-pds.lpl.arizona.edu/PDS/; (McEwen, 2006). (2) CTX: https://pds-imaging.jpl.nasa.gov/volumes/mro.html; (Malin, 2007). (3) MOLA: https://pds-geosciences.wustl.edu/missions/mgs/megdr.html; (Neumann et al., 2003). CaSSIS data are available through the ESA Planetary Science Archive (http://archives.esac.esa.int/psa/#!Table%

20View/CaSSIS=instrument). The CTX DEM mosaic of Oxia Planum is available at https://doi.org/10.21954/ou.rd.16451220.v1. One HiRISE DEM used is available on the HiRISE PDS. All other CTX and HiRISE Digital Elevation Models and shapefiles created for this project are available at https://doi.org/10.6084/m9.figshare.c.6011638.v2.

Acknowledgements

Support from the UK Space Agency is gratefully acknowledged (JMD: ST/R002355/1; ST/V002678/1; ST/W002566/1, MRB: ST/T002913/1, ST/V001965/1; ST/R001413/1, PF; ST/W002736/1). We thank the various Mars instrument science and engineering teams for their consistently excellent and dedicated work. We thank Susan Conway and Axel Noblet for assistance with DEM production. CaSSIS is a project of the University of Bern and funded through the Swiss Space Office via ESA's PRODEX programme. The instrument hardware development was also supported by the Italian Space Agency (ASI) (ASI-INAF agreement no. I/018/12/0), INAF/Astronomical Observatory of Padova, and the Space Research Center (CBK) in Warsaw. Support from SGF (Budapest), the University of Arizona (Lunar and Planetary Lab.) and NASA are also gratefully acknowledged. Operations support from the UK Space Agency under grant ST/R003025/1 is also acknowledged.

Appendix A. Supplementary material

Supplementary material related to this article can be found online at https://doi.org/10.1016/j.epsl.2022.117904.

References

Andrews-Hanna, J.C., 2020. The tectonic architecture of wrinkle ridges on Mars. Icarus 351, 113937. https://doi.org/10.1016/j.icarus.2020.113937.

Balme, M.R., Gupta, S., Davis, J.M., Fawdon, P., Grindrod, P.M., Bridges, J.C., et al., 2020. Aram Dorsum: an extensive mid-Noachian age fluvial depositional system in Arabia Terra, Mars. J. Geophys. Res., Planets 125, e2019JE006244. https://doi.org/10.1029/2019JE006244.

Beyer, R.A., Alexandrov, O., McMichael, S., 2018. The Ames Stereo Pipeline: NASA's open source software for deriving and processing terrain data. Earth Space Sci. 5 (9), 537–548. https://doi.org/10.1029/2018EA000409.

Burr, D.M., Williams, R.M.E., Wendell, K.D., Chojnacki, M., Emery, J.P., 2010. Inverted fluvial features in the Aeolis/Zephyria Plana region, Mars: formation mechanisms and initial paleodischarge estimates. J. Geophys. Res. 115 (E7), E07011. https://doi.org/10.1029/2009JE003496.

Butcher, F.E.G., Balme, M.R., Conway, S.J., Gallagher, C., Arnold, N.S., Storrar, R.D., et al., 2021. Sinuous ridges in Chukhung crater, Tempe Terra, Mars: implications for fluvial, glacial, and glaciofluvial activity. Icarus 357. https://doi.org/10.1016/j.icarus.2020.114131, 114131.

Carter, J., Loizeau, D., Mangold, N., Poulet, F., Bibring, J.-P., 2015. Widespread surface weathering on early Mars: a case for a warmer and wetter climate. Icarus 248, 373–382. https://doi.org/10.1016/j.icarus.2014.11.011.

Ciarletti, V., Clifford, S., Plettemeier, D., Le Gall, A., Hervé, Y., Dorizon, S., et al., 2017. The WISDOM radar: unveiling the subsurface beneath the ExoMars Rover and identifying the best locations for drilling. Astrobiology 17, 565–584. https://doi.org/10.1089/ast.2016.1532.

Coates, A.J., Jaumann, R., Griffiths, A.D., Leff, C.E., Schmitz, N., Josset, J.-L., et al., 2017. The PanCam instrument for the ExoMars rover. Astrobiology 17, 511–541. https://doi.org/10.1089/ast.2016.1548.

Colombera, L., Mountney, N.P., McCaffrey, W.D., 2015. A meta-study of relationships between fluvial channel-body stacking pattern and aggradation rate: implications for sequence stratigraphy. Geology 43, 283–286. https://doi.org/10.1130/G36385.

Davis, J.M., Balme, M., Grindrod, P.M., Williams, R.M.E., Gupta, S., 2016. Extensive Noachian fluvial systems in Arabia Terra: implications for early Martian climate. Geology 44, 847–850. https://doi.org/10.1130/G38247.1.

Davis, J.M., Gupta, S., Balme, M.R., Grindrod, P.M., Fawdon, P., Dickeson, Z.I., Williams, R.M.E., 2019. A diverse array of fluvial depositional systems in Arabia Terra: evidence for mid-Noachian to early Hesperian rivers on Mars. J. Geophys. Res., Planets 124, 1913–1934. https://doi.org/10.1029/2019JE005976.

Favaro, E.A., Balme, M.R., Davis, J.M., Grindrod, P.M., Fawdon, P., Barrett, A.M., Lewis, S.R., 2021. The aeolian environment of the landing site for the ExoMars Rosalind Franklin Rover in Oxia Planum, Mars. J. Geophys. Res., Planets 126, e2020JE006723. https://doi.org/10.1029/2020JE006723.

Fawdon, P., Grindrod, P., Orgel, C., Sefton-Nash, E., Adeli, S., Balme, M., et al., 2021. The geography of Oxia Planum. J. Maps 17, 762–778. https://doi.org/10.1080/17445647.2021.1982035.

Fawdon, P., Balme, M.R., Davis, J.M., Bridges, J.C., Gupta, S., Quantin-Nataf, C., 2022. Rivers and lakes in Western Arabia Terra: the fluvial catchment of ExoMars rover landing site. J. Geophys. Res., Planets 27, e2021JE007045. https://doi.org/10.1029/2021JE007045.

Grant, J.A., Golombek, M.P., Grotzinger, J.P., Wilson, S.A., Watkins, M.M., Vasavada, A.R., et al., 2011. The science process for selecting the landing site for the 2011 Mars science laboratory. Planet. Space Sci. 59 (11–12), 1114–1127. https://doi.org/10.1016/j.pss.2010.06.016.

Grant, J.A., Golombek, M.P., Wilson, S.A., Farley, K.A., Williford, K.H., Chen, A., 2018. The science process for selecting the landing site for the 2020 Mars rover. Planet. Space Sci. 164, 106–126. https://doi.org/10.1016/j.pss.2018.07.001.

Grotzinger, J.P., Sumner, D., Kah, L., Stack, K., Gupta, S., Edgar, L., et al., 2014. A habitable fluvio-lacustrine environment at Yellowknife Bay, Gale Crater, Mars. Science 343, 1242777. https://doi.org/10.1126/science.1242777.

Hayden, A.T., Lamb, M.P., Fischer, W.W., Ewing, R.C., McElory, B.J., Williams, R.M.E., 2019. Formation of sinuous ridges by inversion of river-channel belts in Utah, USA, with implications for Mars. Icarus. https://doi.org/10.1016/j.icarus.2019.04.019.

Kirk, R.L., Howington-Kraus, E., Rosiek, M.R., Anderson, J.A., Archinal, B.A., Becker, K.J., et al., 2008. Ultrahigh resolution topographic mapping of Mars with MRO HiRISE stereo images: meter-scale slopes of candidate Phoenix landing sites. J. Geophys. Res. 113, E00A24. https://doi.org/10.1029/2007JE003000.

Kite, E.S., Sneed, J., Mayer, D.P., Wilson, S.A., 2017. Persistent or repeated surface habitability on Mars during the late Hesperian–Amazonian. Geophys. Res. Lett. 44, 3991–3999. https://doi.org/10.1002/2017GL072660.

Lapôtre, M.G.A., Ielpi, A., Lamb, M.P., Williams, R.M.E., Knoll, A.H., 2019. Model for the formation of single-thread rivers in barren landscapes and implications for pre-Silurian and Martian fluvial deposits. J. Geophys. Res., Earth Surf. 124 (12), 2757–2777. https://doi.org/10.1029/2019JF005156.

Loizeau, D., Mangold, N., Poulet, F., Bibring, J.P., Gendrin, A., Ansan, V., et al., 2007. Phyllosilicates in the Mawrth Vallis region of Mars. J. Geophys. Res. 112 (8), 1–20. https://doi.org/10.1029/2006je002877.

Malin, M.C., 2007. MRO Context Camera experiment data record level 0 v1.0. NASA Planetary Data System. https://doi.org/10.17189/1520266.

Malin, M.C., Bell, J.F., Cantor, B.A., Caplinger, M.A., Calvin, W.M., Clancy, R.T., et al., 2007. Context camera investigation on board the Mars reconnaissance orbiter. J. Geophys. Res. 112, 1–25. https://doi.org/10.1029/2006je002808.

Mandon, L., Parkes Bowen, A., Quantin-Nataf, C., Bridges, J.C., Carter, J., Pan, L., et al., 2021. Morphological and spectral diversity of the clay-bearing unit at the ExoMars landing site Oxia Planum. Astrobiology 21, 464–480. https://doi.org/10.1089/ast.2020.2292.

McEwen, A.S., 2006. MRO Mars high resolution image science experiment RDR V1.0. NASA Planetary Data System. https://doi.org/10.17189/1520303.

McEwen, A.S., Eliason, E.M., Bergstrom, J.W., Bridges, N.T., Hansen, C.J., Delamere, W.A., et al., 2007. Mars reconnaissance orbiter's high resolution imaging science experiment (HiRISE). J. Geophys. Res. 112 (5), 1–40. https://doi.org/10.1029/2005je002605.

McNeil, J.D., Fawdon, P., Balme, M.R., Coe, A.L., 2021. Morphology, morphometry and distribution of isolated landforms in southern Chryse Planitia, Mars. J. Geophys. Res., Planets 126 (5), e2020JE006775. https://doi.org/10.1029/2020JE006775.

Miller, D.M., Dudash, S.L., McGeehin, J.P., 2018. Paleoclimate record for Lake Coyote, California, and the Last Glacial Maximum and deglacial paleohydrology (25 to 14 cal ka) of the Mojave River. In: Starratt, S.W., Rosen, M.R. (Eds.), From Saline to Freshwater: The Diversity of Western Lakes in Space and Time, Special Paper, vol. 536. Geological Society of America, Boulder, CO, pp. 1–20.

Molina, A., López, I., Prieto-Ballesteros, O., Fernández-Remolar, D., de Pablo, M.Á., Gómez, F., 2017. Coogoon Valles, western Arabia Terra: hydrological evolution of a complex Martian channel system. Icarus 293, 27–44. https://doi.org/10.1016/j.icarus.2017.04.002.

Montgomery, D.R., Bandfield, J.L., Becker, S.K., 2012. Periodic bedrock ridges on Mars. J. Geophys. Res., Planets 117 (E3), E03005. https://doi.org/10.1029/2011JE003970.

Murchie, S., Arvidson, R., Bedini, P., Beisser, K., Bibring, J.-P., Bishop, et al., 2007. Compact reconnaissance imaging spectrometer for Mars (CRISM) on Mars reconnaissance orbiter (MRO). J. Geophys. Res. 112, E05S03. https://doi.org/10.1029/2006JE002682.

Neumann, G., Zuber, M., Smith, D.E., 2003. MOLA mission experiment gridded data record. NASA Planetary Data System. https://doi.org/10.17189/1519460.

Noe Dobrea, E.Z., Bishop, J.L., McKeown, N.K., Fu, R., Rossi, C.M., Michalski, J.R., et al., 2010. Mineralogy and stratigraphy of phyllosilicate-bearing and dark mantling units in the greater Mawrth Vallis/west Arabia Terra area: constraints on geological origin. J. Geophys. Res. 115. https://doi.org/10.1029/2009je003351.

Parkes Bowen, A., Bridges, J.C., Tornebene, L., Mandon, L., Quantin-Nataf, C., Patel, M.R., et al., 2022. A CaSSIS and HiRISE map of the Clay-bearing Unit at the ExoMars 2022 landing site in Oxia Planum. Planet. Space Sci. 214, 105429. https://doi.org/10.1016/j.pss.2022.105429.

Quantin-Nataf, C., Carter, J., Mandon, L., Thollot, P., Balme, M., Volat, M., et al., 2021. Oxia Planum: the landing site for the ExoMars "Rosalind Franklin" Rover Mission: geological context and prelanding interpretation. Astrobiology 21. https://doi.org/10.1089/ast.2019.2191.

Silvestro, S., Pacifici, A., Salese, F., Vaz, D.A., Neesemann, A., Tirsch, D., et al., 2021. Periodic bedrock ridges at the ExoMars 2022 landing site: evidence for a changing wind regime. Geophys. Res. Lett. 48 (4), 1–10. https://doi.org/10.1029/2020GL091651.

Stack, K.M., Dietrich, W.E., Lamb, M.P., Sullivan, R.J., Christian, J.R., Newman, C.E., et al., 2022. Orbital and in-situ investigation of periodic bedrock ridges in Glen Torridon, Gale crater, Mars. J. Geophys. Res., Planets 127 (6), 1–33. https://doi.org/10.1029/2021JE007096.

Summons, R.E., Amend, J.P., Bish, D., Buick, R., Cody, G.D., Des Marais, D.J., et al., 2011. Preservation of Martian organic and environmental records: final report of the Mars biosignature working group. Astrobiology 11 (2), 157–181. https://doi.org/10.1089/ast.2010.0506.

Thomas, N., Cremonese, G., Ziethe, R., Gerber, M., Brändli, M., Bruno, G., et al., 2017. The colour and stereo surface imaging system (CaSSIS) for the ExoMars trace gas orbiter. Space Sci. Rev. 212, 1897–1944. https://doi.org/10.1007/s11214-017-0421-1.

Vago, J.L., Westall, F., Pasteur Instrument Teams, Coates, A.J., Jaumann, R., Korablev, O., et al., 2017. Habitability on early Mars and the search for biosignatures with the ExoMars rover. Astrobiology 17, 471–510. https://doi.org/10.1089/ast.2016.1533.

Westall, F., Foucher, F., Bost, N., Bertrand, M., Loizeau, D., Vago, J.L., et al., 2015. Biosignatures on Mars: what, where, and how? Implications for the search for Martian life. Astrobiology 15 (11), 998–1029. https://doi.org/10.1089/ast.2015.1374.

Williams, R.M.E., Irwin, R.P., Zimbelman, J.R., 2009. Evaluation of paleohydrologic models for terrestrial inverted channels: implications for application to Martian sinuous ridges. Geomorphology 107 (3–4), 300–315. https://doi.org/10.1016/j.geomorph.2008.12.015.

Williams, R.M.E., Grotzinger, J.P., Dietrich, W.E., Gupta, S., Sumner, D.Y., Wiens, R.C., et al., 2013. Martian fluvial conglomerates at Gale crater. Science 340, 1068–1072. https://doi.org/10.1126/science.1237317.

Zaki, A.S., Pain, C.F., Edgett, K.S., Castelltort, S., 2021. Global inventory of fluvial ridges on Earth and lessons applicable to Mars. Earth-Sci. Rev. 216. https://doi.org/10.1016/j.earscirev.2021.103561.

Zuber, M.T., Smith, D.E., Solomon, S.C., Muhleman, D.O., Head, J.W., Garvin, J.B., et al., 1992. The Mars Observer laser altimeter investigation. J. Geophys. Res. 97, 7781–7797. https://doi.org/10.1029/92JE00341.